Acta Cryst. (1988). B**44**, 102–107

Crystal Structure and Electron Density of Diammonium Hexaaquacopper(II) Sulfate

BY E. N. MASLEN AND K. J. WATSON

Department of Physics, University of Western Australia, Nedlands, Western Australia 6009, *Australia*

AND F. H. MOORE

Australian Institute of Nuclear Science and Engineering, Lucas Heights, New South Wales 2232, *Australia*

(*Received* 9 *February* 1987; *accepted* 29 *October* 1987)

Abstract

An accurate set of X-ray data collected at 298 K was used to refine the structure and study the deformation density of the title compound $[NH_4]_2[Cu(H_2O)_6](SO_4)_2$, $M_r = 399{\cdot}93$, monoclinic, $P2_1/a$, $a = 9{\cdot}216\ (3)$, $b = 12{\cdot}398\ (3)$, $c = 6{\cdot}301\ (2)$ Å, $\beta = 106{\cdot}12\ (2)°$, $V = 691{\cdot}59$ Å^{-3}, $Z = 2$, $D_x = 1{\cdot}920$ Mg m^{-3}, λ(Mo $K\alpha$) $= 0{\cdot}71069$ Å, $\mu = 1{\cdot}792$ mm^{-1}, $F(000) = 414$, $R = 0{\cdot}044$, $wR = 0{\cdot}019$ for 5007 reflections. A neutron structure confirmed the accuracy of bond lengths reported in an earlier determination. The radial structure of the deformation density near the Cu atom also varies, in a manner correlated with metal–oxygen bond length, and consistent with trends in the isomorphous magnesium and nickel structures. Large differences in bond lengths affected by Jahn–Teller distortion are influenced by interactions with neighbouring groups. The strengths of the metal–oxygen bonds are increased by hydrogen bonding of the ligating water molecules, and decreased by interaction between the oxygen lone pairs and the ammonium group.

Introduction

Maslen, Ridout & Watson (1988) studied the deformation density in the magnesium and nickel members of this series of Tutton's salts. The environment of those metal atoms is approximately octahedral, but more accurately has $4/mmm$ (D_{4h}) symmetry, with one principal axis shorter than the ideal value. The deformation density reflects this departure from the ideal geometry. Minima in the deformation density directed along the short metal–oxygen bonds are 0·3 Å further from the nucleus than those directed along the longer bonds.

The copper member of the series, for which an X-ray structure was reported by Montgomery & Lingafelter (1966), is distorted more strongly than the magnesium and nickel structures because of the Jahn–Teller (1937) effect. The metal is on a centre of symmetry, but its environment, described by three pairs of Cu–O vectors of unequal length, has approximate mmm (D_{2h}) symmetry. This offers the opportunity of studying the effect of distorting the environment of the metal atom on its electron density.

The relationship between the structural geometry and thermal motion in the title compound was studied by Alcock, Duggan, Murray, Tyagi & Hathaway (1984), who determined X-ray structures at 123 and 203 K. Those authors conclude that the structure shows fluxional behaviour, with the CuO_6 chromophore changing dynamically between two different structures, each with approximate D_{4h} symmetry.

Different pairs of Cu–O bonds, corresponding to different axes in the pseudo-octahedron, are elongated in the two structures. The energy difference between them is not large compared with kT, and their occupancy becomes more nearly equal as the temperature rises. This behaviour is compared with those of other CuO_6 systems by Hathaway (1984), and is not considered further in this investigation.

Following a careful room temperature neutron study of the structure, Brown & Chidambaram (1969) expressed concern about extinction in their data, and its possible effect on N–H bond lengths. Those authors were unable to decide whether differences between the X-ray and neutron structures resulted from the redistribution of electron density due to bonding or from errors in the data. A further set of neutron data was collected to resolve this question.

Experimental

Crystals by evaporation from a solution containing stoichiometric quantities of ammonium and copper sulfates in water.

Neutron measurements at 295 K with neutrons of wavelength $\lambda = 0{\cdot}9884$ Å on the four-circle diffractometer at the HIFAR reactor at the Australian Atomic Energy Commission Research Establishment at Lucas Heights, New South Wales. Crystal with six (001), (110) and (1$\bar{1}$0) faces of dimensions 3·73 × 2·92 × 4·73 mm. Neutron cell dimensions determined by least-squares fit to the angular settings of 35 reflections fully centered in the counter aperture:

0108-7681/88/020102-06$03.00

Table 1. *Fractional atomic coordinates and equivalent isotropic thermal parameters*

$B_{eq} = \frac{8}{3}\pi^2 \sum_i \sum_j U_{ij} a_i^* a_j^* \mathbf{a}_i.\mathbf{a}_j$.

	Neutron (×10⁴)				X-ray (×10⁵ N, Cu, O, S; ×10³ H)			
	x	y	z	B_{eq}(Å²)	x	y	z	B_{eq}(Å²)
Cu(1)	0 (–)	0 (–)	0 (–)	1·44	0 (–)	0 (–)	0 (–)	1·52
S(2)	4101 (3)	1389 (2)	7454 (5)	1·76	40965 (3)	13916 (2)	74535 (4)	1·84
O(3)	4151 (2)	2321 (2)	6007 (3)	2·94	41498 (9)	23227 (6)	60012 (12)	3·01
O(4)	5486 (2)	761 (2)	7805 (4)	3·59	54810 (8)	7631 (7)	78064 (15)	3·64
O(5)	2803 (2)	708 (1)	6329 (3)	2·34	27958 (8)	7057 (6)	63256 (12)	2·38
O(6)	3909 (2)	1787 (2)	9573 (3)	2·82	39045 (9)	17877 (6)	95718 (12)	2·85
O(7)	1762 (2)	1165 (2)	1772 (4)	2·79	17477 (10)	11630 (7)	17599 (15)	2·87
O(8)	−1643 (2)	1090 (2)	306 (3)	2·43	−16443 (9)	10860 (7)	3159 (14)	2·52
O(9)	−51 (2)	−654 (2)	2824 (3)	2·05	−468 (9)	−6499 (6)	28203 (11)	2·14
N(10)	1344 (2)	3479 (1)	3597 (2)	2·69	13480 (12)	34837 (9)	35998 (18)	2·71
H(11)	658 (6)	3338 (5)	2112 (8)	6·23	84 (2)	338 (1)	231 (3)	5·69
H(12)	2245 (6)	3001 (4)	4028 (10)	6·47	221 (2)	295 (1)	405 (2)	5·45
H(13)	764 (6)	3349 (5)	4706 (9)	7·57	95 (2)	340 (1)	441 (3)	5·27
H(14)	1683 (6)	4250 (4)	3639 (9)	5·78	173 (2)	422 (2)	356 (3)	7·61
H(15)	2207 (4)	961 (3)	3286 (7)	3·77	211 (1)	96 (1)	288 (2)	2·73
H(16)	2556 (4)	1286 (3)	1074 (6)	3·99	236 (2)	127 (1)	120 (2)	3·24
H(17)	−2673 (4)	951 (3)	−592 (6)	3·34	−249 (2)	98 (1)	−42 (2)	3·31
H(18)	−1416 (4)	1842 (3)	33 (6)	3·47	−155 (2)	170 (1)	12 (2)	3·77
H(19)	−1021 (4)	−596 (3)	3157 (6)	3·53	−82 (2)	−59 (1)	311 (2)	4·04
H(20)	247 (4)	−1406 (3)	3099 (5)	3·06	22 (1)	−128 (1)	304 (2)	2·96

$a = 9{\cdot}218\ (9)$, $b = 12{\cdot}377\ (12)$, $c = 6{\cdot}308\ (6)$ Å, $\beta = 106{\cdot}16\ (7)°$. 2391 reflections within a hemisphere with $(\sin\theta)/\lambda < 0{\cdot}59$ Å^{-1}, $-10 < h < 10$, $0 < |k| < 14$, $0 < l < 7$ measured and reduced by statistical averaging to 1141 unique reflections. Data corrected for absorption using the analytical method with $\mu = 0{\cdot}22$ mm^{-1}, calculated from coefficients by Melkonian (1949) for hydrogen and those by Bacon (1975) for the remaining atoms. $\sigma(I)$ estimated from counting statistics and the probable error in the absorption correction, modified where necessary from a comparison of equivalent reflections. Data-reduction programs by Elcombe, Cox, Pryor & Moore (1971).

Neutron form factors from *International Tables for X-ray Crystallography* (1974). Parameters from full-matrix least-squares minimization of $\sum w(|F_o| - |F_c|)^2$, with $w = 1/\sigma^2(|F_o|)$. Coordinates for atoms in general positions, anisotropic thermal parameters, a scale factor and an isotropic extinction factor refined until $S = 1{\cdot}11$, $R = 0{\cdot}044$, $wR = 0{\cdot}039$, $r^* = 0{\cdot}0244\ (4)$ (Larson, 1970), largest shift $< 0{\cdot}05\sigma$, using programs from the *XRAY*76 system (Stewart, Machin, Dickinson, Ammon, Heck & Flack, 1976).

X-ray diffractometry: Nicolet $P2_1$ diffractometer, graphite-monochromatized Mo $K\alpha$ radiation. Crystal with six (001), (110) and (1$\bar{1}$0) faces of dimensions 0·12 × 0·11 × 0·19 mm. The unit-cell volume is significantly larger than that reported by Brown & Chidambaram (1969), indicating a higher data-collection temperature. 28 377 measured reflections in the range $(\sin\theta)/\lambda < 0{\cdot}953$ Å^{-1}, $0 < |h| < 17$, $0 < |k| < 23$, $-12 < l < 11$, reduced to 5007 unique reflections by statistical averaging. Absorption corrections evaluated by the analytical method with $\mu = 1{\cdot}792$ mm^{-1}. Scale factors calculated from the intensities of six standards, measured every 40 reflections, were generally consistent, with mean values accurate to better than 1%. The total fluctuation in scale factors was 6%, of which the long-term drift accounted for 5%. The $\sigma^2(I)$ values determined from counting statistics were modified for source instability using $\sigma^2(I) = \sigma^2(I)_{initial} + 5{\cdot}6 \times 10^{-5} I^2$, the multiplier for I^2 being derived from the variation of the standard reflections. These estimates of variance were checked with values obtained by comparison of equivalents. The validity of the hypothesis that the two estimates were equal was assessed from the F distribution at the 1% significance level. Five reflections did not meet this criterion. The agreement index $R_{int} = \sum |\Delta(I)| / \sum I$ for the remaining reflections was 0·008.

Atomic scattering factors for H from Stewart, Davidson & Simpson (1965) and for C, Cu, N, O and S, with dispersion corrections from *International Tables for X-ray Crystallography* (1974). A scale factor, isotropic thermal parameters for hydrogen with other structural parameters as in the neutron analysis refined by full-matrix least squares until $S = 2{\cdot}479\ (25)$, $R = 0{\cdot}044$, $wR = 0{\cdot}019$, largest shift $< 0{\cdot}01\sigma$. Data-reduction and structure-refinement programs from the *XTAL*83 system (Stewart & Hall, 1983). No extinction was observed.*

Discussion

The atomic positions are listed in Table 1. Bond lengths and angles calculated from the X-ray and neutron

* Lists of structure factors and anisotropic thermal parameters have been deposited with the British Library Document Supply Centre as Supplementary Publication No. SUP 44482 (24 pp.). Copies may be obtained through The Executive Secretary, International Union of Crystallography, 5 Abbey Square, Chester CH1 2HU, England.

Table 2. *Bond lengths* (Å) *and angles* (°)

	X-ray	Neutron
Cu–O(7)	2·216 (1)	2·228 (2)
Cu–O(8)	2·078 (1)	2·078 (2)
Cu–O(9)	1·962 (1)	1·968 (2)
S(2)–O(3)	1·482 (1)	1·480 (4)
S(2)–O(4)	1·458 (1)	1·459 (4)
S(2)–O(5)	1·481 (1)	1·475 (3)
S(2)–O(6)	1·478 (1)	1·479 (4)
N(10)–H(11)	0·826 (17)	0·988 (5)
N(10)–H(12)	1·014 (16)	0·994 (6)
N(10)–H(13)	0·719 (20)	1·004 (7)
N(10)–H(14)	0·978 (20)	1·004 (6)
O(7)–H(15)	0·738 (13)	0·962 (5)
O(7)–H(16)	0·752 (16)	0·965 (5)
O(8)–H(17)	0·801 (13)	0·976 (4)
O(8)–H(18)	0·782 (14)	0·980 (4)
O(9)–H(19)	0·790 (17)	0·977 (5)
O(9)–H(20)	0·825 (14)	0·974 (4)
O(7)–Cu–O(8)	88·77 (4)	88·86 (8)
O(7)–Cu–O(9)	90·56 (4)	90·63 (9)
O(8)–Cu–O(9)	88·81 (3)	89·04 (8)
O(3)–S(2)–O(4)	109·43 (5)	109·55 (26)
O(3)–S(2)–O(5)	108·19 (5)	108·14 (20)
O(3)–S(2)–O(6)	109·36 (5)	109·12 (23)
O(4)–S(2)–O(5)	108·89 (5)	109·00 (22)
O(4)–S(2)–O(6)	111·03 (5)	111·10 (21)
O(5)–S(2)–O(6)	109·89 (5)	109·88 (25)
H(11)–N(10)–H(12)	110·8 (15)	114·8 (5)
H(11)–N(10)–H(13)	114·5 (18)	107·8 (5)
H(11)–N(10)–H(14)	103·4 (16)	107·8 (5)
H(12)–N(10)–H(13)	102·6 (16)	106·2 (5)
H(12)–N(10)–H(14)	111·0 (14)	109·3 (5)
H(13)–N(10)–H(14)	114·8 (18)	110·9 (5)
Cu–O(7)–H(15)	109·0 (10)	112·2 (3)
Cu–O(7)–H(16)	114·4 (10)	114·3 (3)
H(15)–O(7)–H(16)	108·4 (15)	108·9 (4)
Cu–O(8)–H(17)	117·7 (10)	116·6 (3)
Cu–O(8)–H(18)	119·9 (11)	113·9 (3)
H(17)–O(8)–H(18)	101·5 (13)	106·7 (3)
Cu–O(9)–H(19)	115·0 (10)	114·7 (2)
Cu–O(9)–H(20)	117·8 (10)	118·6 (3)
H(19)–O(9)–H(20)	106·8 (14)	105·1 (3)

Table 3. *Hydrogen-bond distances* (Å) *and angles* (°) *from the neutron structure*

Bond *A*–H···*B*	Distance *A*–*B*	Equivalent position*	Angle *A*–H···*B*
O(7)–H(15)···O(5)	2·821 (3)	x, y, z	170·0 (4)
O(7)–H(16)···O(6)	2·820 (3)	$x, y, z-1$	168·6 (4)
O(8)–H(17)···O(4)	2·708 (3)	$x-1, y, z-1$	177·6 (3)
O(8)–H(18)···O(6)	2·744 (3)	$x-\frac{1}{2}, \frac{1}{2}-y, z-1$	177·2 (4)
O(9)–H(19)···O(5)	2·734 (3)	$-x, -y, 1-z$	171·2 (3)
O(9)–H(20)···O(3)	2·682 (3)	$\frac{1}{2}-x, y-\frac{1}{2}, 1-z$	171·4 (3)
N(10)–H(11)···O(6)	2·901 (2)	$x-\frac{1}{2}, \frac{1}{2}-y, z-1$	164·4 (6)
N(10)–H(12)···O(3)	2·979 (2)	x, y, z	158·1 (5)
N(10)–H(13)···O(3)	3·014 (3)	$x-\frac{1}{2}, \frac{1}{2}-y, z$	157·5 (5)
N(10)–H(13)···O(4)	3·116 (4)	$x-\frac{1}{2}, \frac{1}{2}-y, z$	135·6 (5)
N(10)–H(14)···O(5)	2·869 (2)	$\frac{1}{2}-x, \frac{1}{2}+y, 1-z$	176·7 (5)

* Symmetry operation for the receptor atom *B*.

parameters are listed in Table 2. Other distances and angles relevant to the hydrogen-bond network are given in Table 3. The X-ray and neutron structures are compared in Table 4.

The information obtained by comparing the structure with those of the magnesium and nickel complexes (Maslen, Ridout, Watson & Moore, 1988*a*,*b*) or by comparing X-ray and neutron parameters is limited by their precision. The parameters for the H atoms are less precise than those for the magnesium complex, due in part to the dominance of the Cu atom on the X-ray scattering. The thermal motion is also larger in this case, perhaps due to dynamic Jahn–Teller effects on the Cu atom and its environment. The X-ray data set is not as extensive as that for the magnesium and nickel structures.

Table 4. *Comparison of X-ray* (*X*) *and neutron* (*N*) *structures*

X *N*	Distance (Å)	*X* *N* *N*	Angle (°)
S(2)–S(2)	0·005 (3)	O(7)–O(7)–Cu	28 (9)
O(3)–O(3)	0·004 (2)	O(7)–O(7)–*B*7	160 (10)
O(4)–O(4)	0·005 (2)	O(8)–O(8)–Cu	86 (16)
O(5)–O(5)	0·007 (2)	O(8)–O(8)–*B*8	132 (16)
O(6)–O(6)	0·004 (2)	O(9)–O(9)–Cu	42 (14)
O(7)–O(7)	0·014 (2)	O(9)–O(9)–*B*9	179 (15)
O(8)–O(8)	0·008 (2)	O(3)–O(3)–S(2)	153 (27)
O(9)–O(9)	0·007 (2)	O(4)–O(4)–S(2)	19 (26)
N(10)–N(10)	0·007 (2)	O(5)–O(5)–S(2)	159 (16)
H(11)–H(11)	0·188 (16)	O(6)–O(6)–S(2)	111 (27)
H(12)–H(12)	0·077 (18)	H(11)–H(11)–N(10)	25 (7)
H(13)–H(13)	0·288 (21)	H(12)–H(12)–N(10)	101 (13)
H(14)–H(14)	0·086 (22)	H(13)–H(13)–N(10)	5 (3)
H(15)–H(15)	0·245 (14)	H(14)–H(14)–N(10)	74 (14)
H(16)–H(16)	0·222 (17)	H(15)–H(15)–O(7)	16 (3)
H(17)–H(17)	0·175 (14)	H(16)–H(16)–O(7)	7 (3)
H(18)–H(18)	0·227 (15)	H(17)–H(17)–O(8)	5 (5)
H(19)–H(19)	0·192 (17)	H(18)–H(18)–O(8)	22 (4)
H(20)–H(20)	0·155 (14)	H(19)–H(19)–O(9)	6 (4)
		H(20)–H(20)–O(9)	7 (5)

*B*7, *B*8 and *B*9 are the internal bisectors of the H–O–H angles centred on O(7), O(8) and O(9) respectively.

On the other hand, the X-ray bond lengths for the sulfate group are within 0·001 Å of those in the nickel structure, which is consistent within the limits expected from the standard deviations, supporting their reliability. The neutron bond lengths in this structure are consistent with those obtained by Brown & Chidambaram (1969), and those authors' reservations regarding the effect of systematic error on their positional parameters can be discounted. The mean X-ray N–H and O–H bond lengths are 0·113 (9) and 0·191 (7) Å shorter than the neutron values, the corresponding values for the magnesium complex being 0·162 (7) and 0·216 (5) Å respectively.

The value of the comparison of X-ray and neutron positions for non-H atoms is limited by the accuracy of the neutron structure. The differences between the X-ray and neutron positions for the water oxygens are larger than those for the sulfate oxygens. The *X*–*N* distance of 0·014 (2) Å for O(7), the ligating water oxygen furthest from the copper nucleus, is almost twice those for O(8) and O(9) which are bonded more tightly to the copper. This confirms the trend observed in copper sulfate pentahydrate (Varghese & Maslen, 1985), where the *X*–*N* distance for the space-filling

water of 0·022 Å is larger than the mean value of 0·006 Å for those bonded to the copper. This implies that the closer the approach of a ligating O atom to the metal nucleus, the less well developed is its lone pair system. For ligating N atoms, on the other hand, well developed lone pairs are observed (Maslen & Ridout, 1987).

It is difficult to account for this phenomenon in isolation but when examined in conjunction with the results of Dunitz & Seiler (1983) a consistent trend emerges. Movement of lone-pair electron density into the bonding regions with high electrostatic potential is favoured energetically, as illustrated by the disposition of the nitrogen lone pairs. In the electron-rich environments of bonds between electronegative atoms, however, that movement is inhibited by the Pauli principle, *i.e.* by exchange, which requires that electrons with parallel spins occupy different volume elements. This limits the concentration of oxygen lone-pair density in bonds to transition metals with nearly complete 3*d* subshells.

Indeed it is clear why bonding with electronegative substituents favours removal of an electron from the Cu atom's filled 3*d* subshell. Overlap of the ligating atom's lone pairs with the Cu atom's d^{10} configuration results in a depletion of the 3*d* subshell when the wavefunction is antisymmetrized, generating the $3d^9$ configuration which characterizes Cu^{2+} compounds. Promotion of an electron to an unoccupied state reduces conflict between parallel spins in the same volume element. In the ionic model a promoted 3*d* electron and the diffuse 4*s* valence electron are transferred to neighbouring anions.

In an idealized model of transition-metal bonding all *d* states are exactly degenerate. In practice the degeneracy is approximate. The field due to the ligating groups is not exactly octahedral, and nearby states contribute significantly to the perturbed wavefunction. For a Cu^{2+} ion the energy of the empty 4*s* state is close to that of the 3*d* states. The density for the 4*s* state maximizes further from the nucleus than that for a 3*d* state. A 4*s* contribution to the perturbed wavefunction explains why a Cu^{2+} ion expands as it deforms in the ligand field (Yamatera, 1979). Thus the geometric mean of the Cu—O bond lengths (2·088 Å) is larger than the Ni—O value (2·062 Å), although copper has a greater effective nuclear charge than nickel.

Because of the degeneracy of the *d* states in an ideal octahedral field a single *d* electron or *d* vacancy is unstable, having no resistance to perturbing fields which lower the degeneracy. For this reason the Jahn–Teller distortion is observed quite generally for the $3d^9$ Cu^{2+} structures.

Elongation of a pair of Cu—*X* vectors, related by a centre, is the favoured method of removing the degeneracy of a d^9 configuration in ideal octahedral geometry. One cannot account for this on the basis of a re-population of atomic *d* states alone; the other important factor is the degree of conflict with the Pauli principle which would result from a large reduction in Cu—O bond length.

The principal differences between the copper and nickel structures arise from the changes in the geometry of the hexaaquametal moiety. The hexaaquanickel group, like those for most other metals in the series, has approximate 4/*mmm* symmetry, with *M*—O(9) bonds shorter than *M*—O(7) and *M*—O(8). The reduction in symmetry predicted for the Cu atom by a group theoretical interpretation of the Jahn–Teller theorem would be satisfied by any large distortion with 4/*mmm* symmetry. Cu—O(9) is approximately 0·08 Å shorter than the Ni—O(9) bond in the nickel complex, but removal of the ground-state degeneracy by contraction of the Cu—O(9) bond alone is energetically unfavourable. Whereas Cu—O(8) is similar to Ni—O(8) in length the largest difference between the structures is the 0·14 Å elongation of the Cu—O(7) bond. We understand why this extension is preferred, but for complete understanding we must also determine why that extension relates to O(7) rather than to O(8).

Deformation density

Sections of the difference density $\Delta\rho$, each containing the Cu atom and two of the three non-equivalent pairs of water O atoms, are shown in Fig. 1. Because the calculated structure factors were based on atomic scattering factors, $\Delta\rho$ approximates the true deformation density which is the redistribution of electron density due to chemical bonding. Atomic charges, determined by the method of Hirshfeld (1977) using the program *PARTN* (Chantler, 1985), are given in Table 5. The standard deviations were derived by approximating the density distribution for each atom by that in a sphere of equivalent volume, following the method of Davis & Maslen (1978).

The electron density along the Cu—O bonds is strongly depleted, as is consistent with the Pauli exclusion principle. The electron densities from the filled 3*d* subshell and the lone-pair electron density from the water oxygen overlap. Depletion of the electron density along the line of the *M*—O bond is a necessary consequence of antisymmetrizing the wavefunction. This depletion is especially strong for copper, as expected because its 3*d* subshell is nearly complete. This explains why the atom carries a larger positive charge (0·4 electrons).

Allowing for the lower resolution and stronger depletion of density there is close similarity between Fig. 1(*b*) and the corresponding map for the nickel complex (Maslen, Ridout & Watson 1988). The minimum near the copper, and directed towards O(9) is deeper than and further from the copper nucleus than the minima along Cu—O(7) and Cu—O(8).

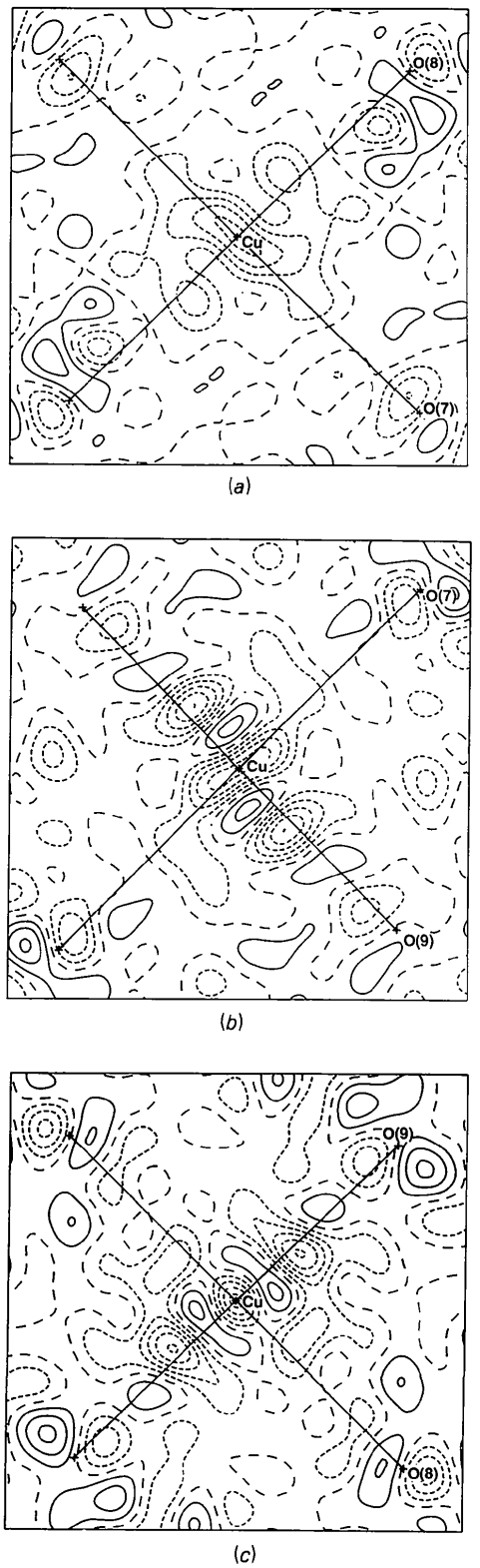

Fig. 1. Residual density for (*a*) the Cu–O(7)–O(8) plane, (*b*) the Cu–O(7)–O(9) plane and (*c*) the Cu–O(8)–O(9) plane. Contour interval 0·15 e Å^{-3}. Zero contour broken. Negative contours dotted.

Table 5. *Atomic charges, as defined by Hirshfeld* (1977)

Atom	Group	Charge	Atom	Group	Charge
Cu		0·41 (3)	N(10)		0·32 (2)
O(7)		−0·10 (2)	H(11)		0·26 (2)
H(15)		−0·02 (2)	H(12)		0·15 (2)
H(16)		0·08 (2)	H(13)		0·15 (2)
	H_2O	−0·04	H(14)		0·11 (2)
O(8)		−0·11 (2)		NH_4	0·99
H(17)		0·01 (2)	S(2)		0·17 (2)
H(18)		0·04 (2)	O(3)		−0·40 (2)
	H_2O	−0·06	O(4)		−0·51 (2)
O(9)		0·08 (2)	O(5)		−0·34 (2)
H(19)		0·12 (2)	O(6)		−0·16 (2)
H(20)		−0·07 (2)		SO_4	−1·22
	H_2O	0·13			
	$Cu(H_2O)_6$	0·46			

The relationship between the geometry and the characteristics of the deformation density peculiar to O(9) is described by Maslen, Ridout & Watson (1988). The atoms O(7) and O(8) are respectively 3·153 (3) and 3·188 (3) Å from the ammomium group. The Cu–O(7)–N(10) and Cu–O(8)–N(10) angles are 128·8 (1) and 137·7 (1)° respectively, and the orientation of the water oxygen lone pairs not involved in the Cu–O bond favours interaction with the ammonium group. This is not true for the O(9) water, for which the O(9)–N(10) distance is 3·692 (2) Å. This asymmetry accounts for a reduction from octahedral to 4/*mmm* symmetry in the nickel structure.

This approach of the ammonium ion towards the ligating waters containing O(7) and O(8) lengthens the Cu–O bond and increases the electron density along the line of the *M*–NH_4 interaction. This accounts for the lesser depletion of electron density along the *M*–O(7) and *M*–O(8) bonds, and also for the qualitative change in the nature of the depletion, which is strongest further from the nucleus in the case of *M*–O(9).

Although Figs. 1(*a*) and 1(*c*) are broadly similar to the corresponding nickel maps, the densities near the Cu–O(7) and Cu–O(8) bonds resemble one another less closely than those in the nickel structure. The approximate 4*m* symmetry of the O(7)–Ni–O(8) map is less obvious in the copper complex. This is expected since the Cu–O(7) and Cu–O(8) bonds differ in length, whereas Ni–O(7) and Ni–O(8) are similar. A detailed examination indicates the degree of polarization near the copper to be correlated inversely with the Cu–O bond length. To this extent the symmetry of the deformation density is consistent with the geometry.

While the main characteristics of the structure and density relevant to O(9) have been explained, the reason for the difference between O(7) and O(8) is less obvious. A careful study was made of all the interactions in the structure which could influence the hexaaquacopper moiety, the study extending to the second and then to the third coordination spheres. The distribution of the more distant interactions does not reveal marked anisotropy of a type which would account for the difference between O(7) and O(8).

However, as noted by Brown & Chidambaram (1969), there is a small but distinct difference between the hydrogen-bond network involving these atoms, as is evident from Table 3.

Both hydrogen bonds from the water molecules are linked to sulfate oxygens, but the hydrogen bonds linking O(7) to O(5) and O(6) are relatively long, with unfavourable geometries and a large O(5)···O(7)··· O(6) angle [118·04 (6)°]. The O(7)–H(15)···O(5) and O(7)–H(16)···O(6) interactions may be weakened by competition with the stronger N(10)–H(14)···O(5) and N(10)–H(11)···O(6) hydrogen bonds, as is seen from Table 3. O(8), on the other hand, is the donor atom for a strong hydrogen bond to O(4), which is an acceptor only for one other very weak bifurcated bond, from N(10)–H(13). It appears that this difference in hydrogen-bond strengths is sufficient to differentiate between the Cu–O(7) and Cu–O(8) vectors, determining their behaviour under Jahn–Teller distortion.

This is suggested by the work of Brown & Chidambaram (1969), but was not pressed by those authors because the hydrogen-bond lengths involving O(9) are so similar to those for O(8). A difference between O(9) and O(8) was regarded as necessary to explain the shorter length of the Cu–O(9) bond, which is characteristic of the Tutton's salt series. That shortening is related to O(9)'s interactions with the ammonium groups, and not to its hydrogen-bond interactions, as explained above.

Thus both the bond-length trends in the structure, and the topography of the deformation density, are consistent with a model for transition-metal bonding in which a water molecule's ligating power is increased by strong hydrogen bonding of its own hydrogens. That ligating power is decreased by competitive interaction between the water oxygen's lone pair and the ammonium group.

Financial support was received from the Australian Institute for Nuclear Science and Engineering and the Australian Research Grants Scheme. Thanks are due to B. W. Skelton, who prepared the crystals for this work, to A. H. White for assistance with the X-ray data and to the AINSE Neutron Diffraction Group for assistance with neutron diffraction facilities.

References

ALCOCK, N. W., DUGGAN, M., MURRAY, A., TYAGI, S. & HATHAWAY, B. J. (1984). *J. Chem. Soc. Dalton Trans.* pp. 7–14.

BACON, G. E. (1975). *Neutron Diffraction,* p. 39. Oxford: Clarendon Press.

BROWN, G. M. & CHIDAMBARAM, R. (1969). *Acta Cryst.* B**25**, 676–687.

CHANTLER, C. (1985). *PARTN* program – listing and documentation. Unpublished work.

DAVIS, C. L. & MASLEN, E. N. (1978). *Acta Cryst.* A**34**, 743–746.

DUNITZ, J. D. & SEILER, P. (1983). *J. Am. Chem. Soc.* **105**, 7056–7058.

ELCOMBE, M. M., COX, G. W., PRYOR, A. W. & MOORE, F. H. (1971). *Programs for the Management and Processing of Neutron Diffraction Data.* AAEC Report TM578. Australian Atomic Energy Commission, Lucas Heights, New South Wales, Australia.

HATHAWAY, B. J. (1984). *Struct. Bonding (Berlin)*, **57**, 55–118.

HIRSHFELD, F. (1977). *Theor. Chim. Acta,* **44**, 129–138.

International Tables for X-ray Crystallography (1974). Vol. IV. Birmingham: Kynoch Press. (Present distributor D. Reidel, Dordrecht.)

JAHN, H. A. & TELLER, E. (1937). *Proc. R. Soc. London Ser. A,* **161**, 220–235.

LARSON, A. C. (1970). *Crystallographic Computing,* edited by F. R. AHMED, pp. 209–213. Copenhagen: Munksgaard.

MASLEN, E. N. & RIDOUT, S. C. (1987). B**43**, 352–356.

MASLEN, E. N., RIDOUT, S. C. & WATSON, K. J. (1988). *Acta Cryst.* B**44**, 96–101.

MASLEN, E. N., RIDOUT, S. C., WATSON, K. J. MOORE, F. H. (1988*a*). *Acta Cryst.* C**44**, 409–412.

MASLEN, E. N., RIDOUT, S. C., WATSON, K. J. & MOORE, F. H. (1988*b*). *Acta Cryst.* C**44**, 412–415.

MELKONIAN, E. (1949). *Phys. Rev.* **76**, 1750–1759.

MONTGOMERY, H. & LINGAFELTER, E. C. (1966). *Acta Cryst.* **20**, 659–662.

STEWART, J. M. & HALL, S. R. (1983). *The XTAL System of Crystallographic Programs.* Tech. Rep. TR-1364. Computer Science Centre, Univ. of Maryland, College Park, Maryland, USA.

STEWART, J. M., MACHIN, P. A., DICKINSON, C. W., AMMON, H. L., HECK, H. & FLACK, H. (1976). The *XRAY*76 system. Tech. Rep. TR-446. Computer Science Centre, Univ. of Maryland, College Park, Maryland, USA.

STEWART, R. F., DAVIDSON, E. R. & SIMPSON, W. T. (1965). *J. Chem. Phys.* **42**, 3175–3187.

VARGHESE, J. N. & MASLEN, E. N. (1985). *Acta Cryst.* B**41**, 184–190.

YAMATERA, H. (1979). *Acta Chem. Scand. Ser. A,* **33**, 107–111.